

[2]

EXPERIMENTAL STUDIES IN NATURAL GROUNDWATER-RECHARGE DYNAMICS: THE ANALYSIS OF OBSERVED RECHARGE EVENTS

MARIOS SOPHOCLEOUS and CHARLES A. PERRY

Kansas Geological Survey, University of Kansas, Lawrence, KS 66046 (U.S.A.)
U.S. Geological Survey, Lawrence, KS 66046 (U.S.A.)

(Received November 24, 1984; revised and accepted May 29, 1985)

ABSTRACT

Sophocleous, M. and Perry, C.A., 1985. Experimental studies in natural groundwater-recharge dynamics: The analysis of observed recharge events. *J. Hydrol.*, 81: 297–332.

The amounts and time distribution of groundwater recharge from precipitation over an approximately 19-month period were investigated at two instrumented sites in south-central Kansas. Precipitation and evapotranspiration sequences, soil-moisture profiles and storage changes, water fluxes in the unsaturated zone and hydraulic gradients in the saturated zone at various depths, soil temperatures, water-table hydrographs, and water-level changes in nearby wells clearly depict the recharge process.

Antecedent moisture conditions and the thickness and nature of the unsaturated zone were found to be the major factors affecting recharge. Although the two instrumented sites are located in sand-dune environments in areas characterized by shallow water table and subhumid continental climate, a significant difference was observed in the estimated effective recharge. The estimates ranged from less than 2.5 to approximately 154 mm at the two sites from February to June 1983. The main reasons for this large difference in recharge estimates were the greater thickness of the unsaturated zone and the lower moisture content in that zone resulting from lower precipitation and higher potential evapotranspiration for one of the sites. Effective recharge took place only during late winter and spring. No summer or fall recharge was observed at either site during the observation period of this study.

INTRODUCTION

Quantification of groundwater recharge is a major problem in many water-resource investigations. The conventional method of estimating recharge as precipitation minus evapotranspiration minus runoff, with allowance for changes in soil-moisture storage, is very sensitive to measurement errors and to the time scale of analysis and often leads to an underestimation of recharge (Howard and Lloyd, 1979). To avoid compounding errors in the hydrologic budget, an effort was undertaken to obtain direct estimates of vertical water fluxes at or near the water table. This approach involves a detailed study of the unsaturated–saturated flow system. However,

the problem of spatial variability of recharge remains complex, and the above-mentioned unsaturated—saturated approach may be impractical for regional applications given the present state of technology.

In order to avoid the problem of spatial variability of groundwater recharge, its areal structure was decoupled from its time distribution, thus simplifying the recharge-estimation problem to the one of determination of time distribution and amounts at two experimental recharge sites in south-central Kansas. The sites are located in dune-sand areas of moderate precipitation and negligible runoff, which are considered favorable environments for natural groundwater recharge. Emphasis was given to investigating the mechanisms of precipitation-related, natural groundwater recharge by direct measurements within the unsaturated—saturated flow regime.

The approach followed in this study is similar to that followed by Freeze and Banner (1970), which is to chart the transport of moisture from the surface through the unsaturated zone, across the water table, and into the saturated groundwater-flow system. Such a profile of groundwater recharge would consist of charting the following items: (a) precipitation; (b) potential or actual evapotranspiration; (c) soil-moisture content at various depths; (d) change in soil-moisture storage in the unsaturated soil profile; (e) water fluxes at the deepest tensiometer-crest level above the water table and at or in the immediate vicinity of the water table; (f) soil-temperature anomalies due to the recharging-water influxes; (g) water-table hydrograph; (h) saturated water fluxes or hydraulic gradients near the water table and deeper in the groundwater-flow system; and (i) water-level changes in the general area of the recharge sites.

Background information for recharge profiles would include soil-texture profiles, water-characteristic curves (that is, the relationship between capillary-pressure head and soil-moisture content), and hydraulic—conductivity functions.

In this study groundwater recharge was defined as “effective recharge”; that is, that water that percolates into the lower limits of the unsaturated zone, reaches the water table, and *causes measurable water-table rise*. This definition was extended to include amounts of recharge for maintaining water-table rises *already achieved from an immediately preceding effective-recharge event*.

Hydrogeology of the recharge sites

One of the recharge sites (Fig. 1), the Burrton site, overlies the Equus Beds aquifer, while the other one, the Zenith site, overlies the Great Bend aquifer of south-central Kansas. Both aquifers, considered part of the regional High Plains aquifer, are used extensively for irrigated agricultural production, although the Equus Beds aquifer also is used to support significant water needs of the city of Wichita, Kansas. Both the Burrton and Zenith recharge sites are located in relatively flat, low-relief sand-dune environments (Fig. 1).

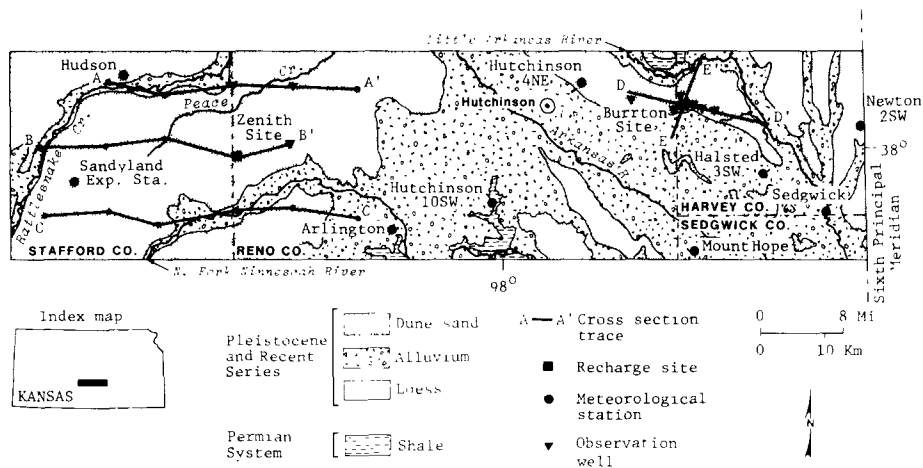


Fig. 1. Generalized surficial geology of the study area (adapted from Kansas Geological Survey, 1964).

No established drainage pattern exists, indicating that surface runoff may be negligible. Rainfall either infiltrates directly into the sandy soil or accumulates in shallow depressions. The sites are covered by native mixed-grass vegetation.

A generalized surficial geology map of the area is shown in Fig. 1. The study sites consist of unconsolidated deposits of predominantly Holocene and Pleistocene age overlying Permian bedrock. The unconsolidated deposits are of fluvial origin and consist of gravel, sand, silt, and clay in various proportions. The sand and gravel beds generally lie between lenses of silt, clay, and sandy clay as can be inferred from the natural gamma logs at each of the recharge sites (Fig. 2). Significant clay layers can be recognized at 19–21 and 23–25 m depth levels for the Burrton site and at the 25–33 m depth level for the Zenith site (Fig. 2). For the most part, the fluvial deposits are covered by eolian deposits. A large sand-dune deposit, mostly underlain by discontinuous clay lenses, occurs in the area of the recharge sites (Fig. 1). The soil at the sites belongs to the Pratt series, which consists of deep, well-drained, gently undulating soils. These soils were formed in sandy eolian deposits and exhibit low available water capacity (Rockers et al., 1966).

Approximate directions of groundwater flow along the cross-sections shown in Fig. 1 are depicted in Figs. 3 and 4. These cross-sections were drawn parallel to the general direction of flow so as to depict true gradients. The hydraulic-head data for the Burrton area (Fig. 3) were compiled for 1978–1981 because of a lack of complete data for any single time. The hydraulic-head data for the Zenith area (Fig. 4) were determined from water levels measured in piezometer nests and wells during March 1982. Based on these data, equipotential lines were drawn, and principal directions of groundwater flow were indicated. From these and other more localized

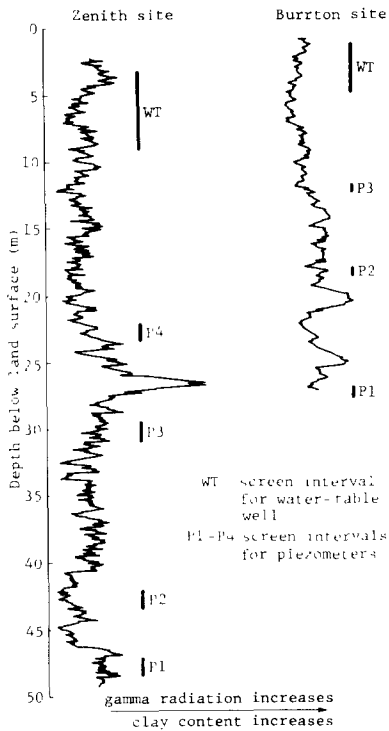


Fig. 2. Natural gamma logs and piezometer-screen intervals for Zenith and Burrton recharge sites.

cross-sectional flow nets, both the Burrton and Zenith sites were identified as being groundwater-recharge sites (with groundwater moving downwards away from the water table).

Hydrometeorological setting

The climate at the study sites is characterized by moderate precipitation, a wide range of temperatures, and moderately high average wind velocity. The normal annual precipitation is approximately 738 mm. The amount of precipitation, however, varies greatly from year to year and generally increases eastwards. The lowest average precipitation for any one month is 18.5 mm during January, and the highest average is 113.3 mm during May. Approximately 72% of the annual amount of precipitation falls from April to September (Rockers et al., 1966). Much of the precipitation usually falls as heavy rains followed by periods of deficient rainfall. Snowfall varies from year to year, but the average annual amount is approximately 508 mm.

Normal monthly mean temperatures range from low during January of -0.5°C to a high in July of 26.8°C . The annual mean temperature is 13.4°C . The prevailing winds are southerly, with average wind speeds of approximately

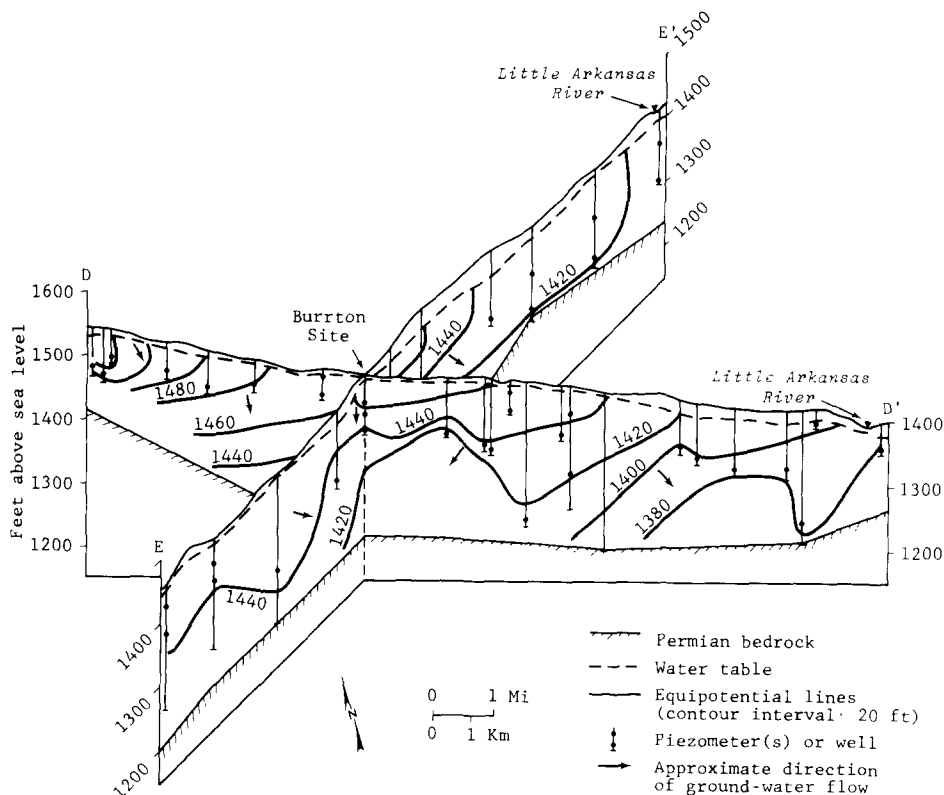


Fig. 3. Cross-sections in vicinity of Burrton site depicting 1978–1981 approximate directions of groundwater flow. To convert values in ft to m, multiply by 0.305.

20 km h^{-1} . The rate of evaporation from a free-water surface is approximately 1397 mm during the period from April to October (Rockers et al., 1966).

Instrumentation

The instrumentation employed at each of the two recharge sites is diagrammed in Fig. 5 (from Sophocleous and Perry, 1984). The purpose of the instrumentation was to provide integrated measurements of subsurface flow on a year-round basis. Data collection was automated as much as possible by using battery-operated programmable data loggers, which recorded data on magnetic cassettes on an hourly and daily basis at each site. Through a cassette reader these data were transferred to the office computer for processing. For further details on the data-collection effort, instrument calibration, and evaluation, the reader is referred to Sophocleous and Perry (1984). In addition to the automated data collection, neutron-moisture readings, as well as piezometer-nest, gypsum-block, and tensiometer readings,

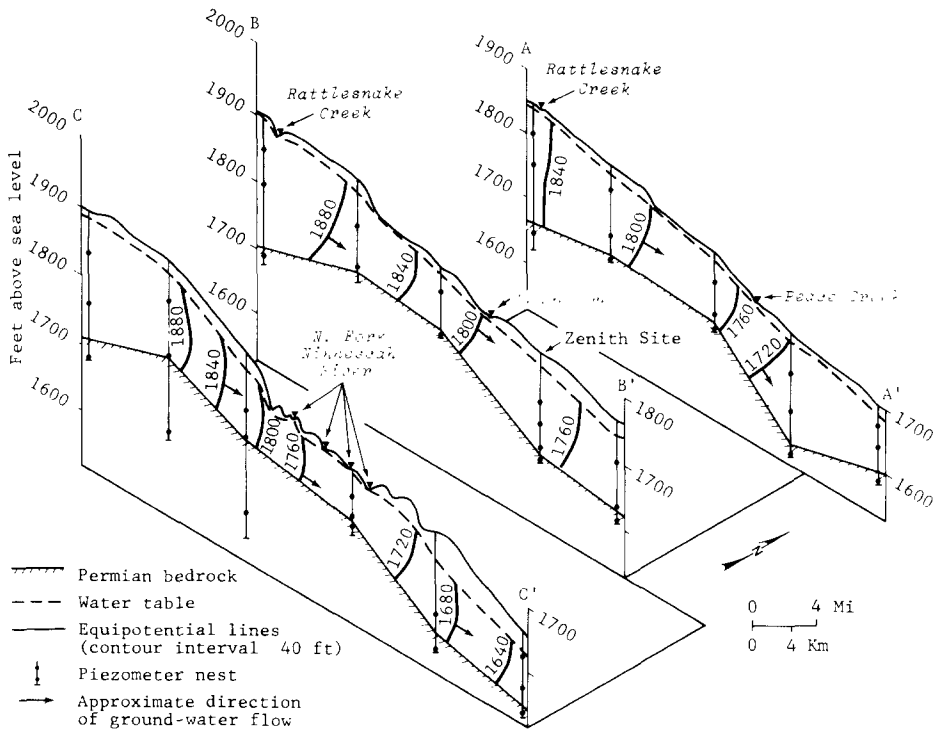


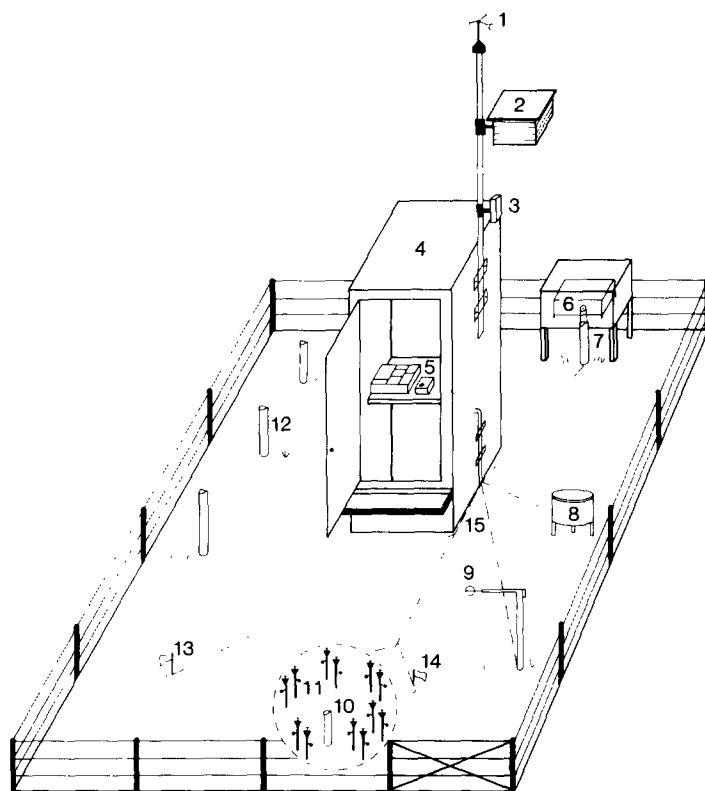
Fig. 4. Cross-sections in vicinity of Zenith site depicting 1982 approximate directions of groundwater flow. To convert values in ft to m, multiply by 0.305.

were made manually on a weekly basis by observers. Both sites were instrumented during June 1982, and data collection was continued until December 1983. Table 1 shows the onsite and laboratory measurements and the instruments or techniques used for such measurements. All laboratory analyses were conducted at the Kansas Geological Survey porous-media laboratory under the direction of the senior author.

The piezometer nest for the Burrton site consisted of three piezometers (Fig. 2), the shallowest one (P3) screened at 12 m in sand, the next (P2) at 17 m in clayey sediments above a clay layer, and the deepest one (P1) at 27 m just below a clay layer. The piezometer nest for the Zenith site consisted of four piezometers (Fig. 2), the shallowest one (P4) screened at 23 m in sand, the next (P3) at 31 m in silty clay, the next (P2) at 43 m in sand and clay, and the deepest one (P1) at 48 m in red shale (bedrock). These piezometers were already in place at the start of this study as part of a water-quality-monitoring program.

METHODOLOGY

The customary method of calculating groundwater recharge by multiplying a constant specific-yield value by the water-table rise over a certain



NOT TO SCALE

Fig. 5. Diagram showing instruments at a site (1 = anemometer; 2 = temperature and relative-humidity sensors; 3 = barometer; 4 = housing unit; 5 = data loggers; 6 = water-level recorder; 7 = water-table well; 8 = precipitation gage; 9 = net radiometer; 10 = neutron-probe access tube; 11 = tensiometer nest; 12 = piezometer nest; 13 = thermocouple hole; 14 = gypsum blocks; 15 = underground connecting lines).

time interval may be erroneous, especially in shallow aquifers (Duke, 1972; Sophocleous, 1985). Therefore, vertical water fluxes were calculated by employing Darcian approaches in combination with water-balance equations as described in the methods below:

(1) By measuring the vertical hydraulic gradient based on tensiometer readings and multiplying that gradient by the corresponding unsaturated hydraulic conductivity. However, because of hysteresis effects and frequent tensiometer malfunctions, this method was used only for providing support in doubtful cases or for backup data for filling in gaps in method 2.

(2) By obtaining an "average" field-water-characteristic curve from concurrent tensiometer and neutron readings for certain depth intervals. The hydraulic gradient then was determined from that curve by determining the hydraulic-head values corresponding to the measured neutron-moisture contents, θ , at the required depths. Finally, that gradient was multiplied by the appropriate hydraulic-conductivity function, $K(\theta)$, to obtain the water

TABLE 1
Experimental measurements

Measurement	Instrument or technique
<i>Onsite data — atmospheric</i>	
precipitation	tipping-bucket rain gauge
atmospheric pressure	barometric-pressure transducer
air temperature	thermistor probe
relative humidity	relative-humidity probe
wind speed	anemometer
net radiation	Fritchen-type net radiometer
<i>Onsite data — subsurface^a</i>	
hydraulic head	piezometer and duplicate tensiometer nests
water table	water-table well
soil-moisture content	neutron probe, gravimetric method, and gypsum blocks
bulk density	gamma probe and core method
soil temperature	thermocouples
<i>Laboratory data^a</i>	
Soil texture	hydrometer method
particle density	pycnometer method
bulk density	clod method
water characteristic	hanging column, pressure plate, pressure membrane
hydraulic conductivity	constant-head permeameter, water-characteristic-based methods

^aMajor references: Black, 1965; ASTM, 1979.

flux at the required depth interval. The average soil-water-characteristic curve is found advantageous over direct tensiometer readings for several reasons: (a) it averages hysteresis effects, since it is the mean of the wetting and drying field curves; (b) it avoids tensiometer failures due to leakage, freezing, etc.; and (c) neutron readings, upon which this method is based, are more reliable for a long-term record than are tensiometer readings. The $K(\theta)$ function, in turn, was estimated based on the saturated hydraulic-conductivity value and the water-characteristic curve. For this purpose, several of the already well-established procedures were employed, such as those of Millington and Quirk (1959, 1961), Jackson et al. (1965) and that of Brooks and Corey (1964), as will be explained later.

(3) However, both above-mentioned methods 1 and 2 could estimate only the moisture fluxes up to the depth of the deepest tensiometer; i.e., up to 1.2 m at Burrton and 1.5 m at Zenith. In order to obtain the water flux at the water table for the case where the water table was significantly below the depth of the deepest tensiometers, a water-balance equation for the soil profile was employed. This procedure is based on periodic moisture-content measurements along the soil profile (Rose et al., 1965; Van Bavel et al., 1968). From the one-dimensional (vertical) form of the water-balance equation:

$$\frac{\partial \theta}{\partial t} = - \frac{\partial q}{\partial z} \quad (1)$$

assuming negligible lateral soil-moisture flow, one obtains by integration from depth z to depth $z + dz$:

$$q_z = q_{z+dz} + \int_z^{z+dz} \frac{\partial \theta}{\partial t} dz \quad (2)$$

where q_z is the vertical component of the Darcian water flux (cm per day, positive in the upwards direction), θ is the volumetric water content (cm^3 of water per cm^3 of soil), and t is time (days).

A computer program was written to solve this equation by dividing the subsurface profile down to the water-table position into N layers of thickness Δz_i . The most critical aspect in applying this procedure is that the water flux at a particular depth must be known, and this may not be easy to determine.

To avoid this difficulty the zero-flux plane method was employed (Kimball and Jackson, 1975). This method is based on locating the point of zero hydraulic gradient and thus the zero reference flux in the soil profile, and then summing up the changes in water content above or below that point. However, this method has the disadvantage that, during periods of high recharge, the hydraulic gradient is not zero anywhere in the unsaturated profile, as can be seen in Fig. 6. Thus, the zero-flux plane method could not be used under these conditions. Therefore, the Darcian flux, based on method (2) described above, was used as the reference flux in applying the water-balance eqn. (2) to calculate the flux at the water table for the Zenith site. For the Burrton recharge site, eqn. (2) was not employed because the shallow depth to water table was within the range of the tensiometers.

Application of the above-mentioned methods depends on the success of accurately determining the hydraulic-conductivity function, $K(\theta)$, which is one of the most difficult parameters to determine directly in the field. In addition, the $K(\theta)$ function is one of the most spatially variable parameters (Warrick and Nielsen, 1980) compounding the measurement problem. To overcome some of the parameter-estimation problems, a number of techniques to predict the $K(\theta)$ function were employed. These techniques are based on relatively easily measured parameters, such as the saturated hydraulic conductivity, measured using the constant-head method (Table 1), and water-characteristic curves. These curves were determined using the hanging-column method for low pressures up to 0.25 bar, the pressure plate apparatus for up to 5 bar pressures, and the pressure membrane apparatus for up to 15 bar pressures (Table 1).

Because of the unconsolidated nature of the sandy deposits, continuous undisturbed core samples could not be obtained from either recharge site. Therefore, all soil analyses were performed on disturbed samples, which were compacted to onsite bulk density as determined using the combination

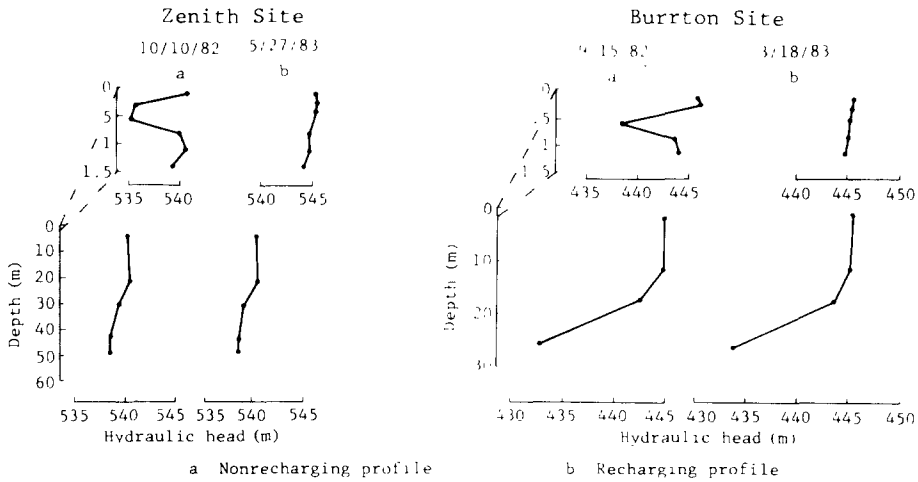


Fig. 6. Hydraulic-head profiles for nonrecharging and recharging periods at Zenith and Burrton recharge sites.

neutron/density probe (Sophocleous and Perry, 1984). Nielsen's et al. (1973) computer program for calculating the $K(\theta)$ function, using the methods of Childs and Collis-George (1950), Marshall (1958), Millington and Quirk (1959, 1961), and Kunze et al. (1968), was suitably modified, and the Brooks and Corey (1964) method was added to it (Shaukat and Sophocleous, 1983). The number of pore classes used (obtained by dividing the water-characteristic curve into a number of volumetric-moisture and pressure-head intervals) for all such determinations was 16.

Evaluation of the above-mentioned five different methods versus measured data from the literature (Shaukat and Sophocleous, 1983) indicated that the Brooks and Corey (1964) method most closely approximated the measured values, although other methods, such as the one of Millington and Quirk (Millington and Quirk, 1959, 1961; Jackson et al., 1965) performed nearly as well. The Brooks and Corey (1964) method was adopted in this study. The fact that the soils at the recharge sites are sandy makes the choice of the above-mentioned capillary flow-based approaches for calculating the $K(\theta)$ function appropriate. Also, the fact that the $K(\theta)$ function is used to calculate reference fluxes at some appreciable soil depth (1.2–1.5 m), where the observed moisture contents were not as dry as the near-surface soils, makes the estimation of the $K(\theta)$ function approach more meaningful.

Potential evapotranspiration (PET) at the recharge sites was estimated in order to better explain observed moisture distributions in the soil profile during different time periods, especially the occurrence or nonoccurrence of recharge, as well as its relative amounts. PET was calculated using the combination methods of Penman (Penman, 1948, 1963) and of Van Bavel-Businger (Van Bavel, 1966) and the radiation method of Jensen and Haise

(1963). In a comprehensive comparison of measured and estimated evapotranspiration values using 16 different methods, it was concluded (Jensen, 1973) that for inland, semiarid environments the Van Bavel-Businger method (with a roughness parameter of $z_0 = 0.25$ cm) and the Jensen-Haise method provided the best estimates of PET, while the Penman method provided the second-best estimate. Because net radiation was measured at the recharge sites, a correlation was determined between the measured net radiation and total solar radiation measured at the Sandyland Experiment Station (25 km west of the Zenith site, Fig. 1) for use in a Jensen-Haise method. The linear-regression equation developed using a sample of 126 daily values is as follows:

$$R_s = 92.2750 + 1.4003R_n \quad (3)$$

with a correlation coefficient of 0.86; where R_s (ly per day) is the total solar radiation, and R_n (ly per day) is the net radiation. A computer program was written to solve the potential-evapotranspiration equations listed in Table 2. All PET estimates from eqns. (4) to (6) in Table 2 were calculated in ly per day and then converted to equivalent depth of evaporation by assuming that the latent heat of vaporization of water is 585 cal g^{-1} . The daily soil-heat flux, G , was considered negligible in this study because it is usually very small, and it tends to average out over a 24-h period.

Comparison of potential-evapotranspiration estimates using the combination and radiation methods mentioned previously showed that for both sites the Jensen-Haise evapotranspiration estimates were mostly lower than the Penman and Van Bavel-Businger estimates, both of which were reasonably close to each other, as shown in Fig. 7. The reason for the closeness of the Penman and Van Bavel-Businger estimates lies in the fact that both formulations are similar in that net radiation and wind effects (eqns. (4) and (5) of Table 2) are explicitly taken into account, while the Jensen-Haise estimate does not explicitly consider wide effects. The higher the wind speed, the larger is the observed discrepancy between the Jensen-Haise estimate on the one hand, and the Penman and Van Bavel-Businger estimates, on the other.

SOIL HYDROGEOLOGIC PROPERTIES AT THE RECHARGE SITES

The Burrton site is located in a light-colored fine-sandy loam soil. The depth variation of soil-particle sizes, the corresponding soil textures, and the saturated hydraulic conductivities for the Burrton site are shown in Fig. 8. The water table at the Burrton site is much shallower and more variable with time than at the Zenith site, with the depth to water averaging approximately 1.2–1.5 m. The Zenith site is situated in a soil that is similar to the Burrton site. The depth variation for the Zenith site of the same properties depicted in Fig. 8 is shown in Fig. 9. The depth to the water table is approximately 5.2 m. This difference in depth to water table between

TABLE 2
Evapotranspiration equations

$$ET_P = \frac{\Delta}{\Delta + \gamma} (R_n + G) + \frac{\gamma}{\Delta + \gamma} 15.36(1.0 + 0.0062 u_2) (e_z^o - e_z) \quad [4]$$

(Penman)

$$ET_{VB-B} = \frac{\Delta}{\Delta + \gamma} (R_n + G) + \frac{\gamma}{\Delta + \gamma} \frac{0.622 \lambda p k^2}{P} \frac{u_z}{\ln(z/z_o)^2} (e_z^o - e_z) \quad [5]$$

(van Bavel-Businger)

$$ET_{J-H} = C_T (T - T_x) R_s \quad [6]$$

(Jensen-Haise)

where

Δ = change in saturation vapor pressure with temperature (mb/°C);

$\gamma = \frac{c_p P}{0.622 \lambda}$ = psychrometer constant (mb/°C);

P = atmospheric pressure (mb);

λ = latent heat of vaporization of water (cal/gm);

c_p = specific-heat capacity of air at constant pressure (cal/gm/°C);

R_n = net radiation (ly/day);

G = heat conducted to soil surface (ly/day);

u_2 = wind speed at 2 m from ground (km/day);

e_z^o = saturation vapor pressure at height z (mb);

e_z = vapor pressure at height z (mb);

ρ = density of air (gm/cm³);

k = von Karman constant (=0.41);

u_z = wind speed at height z (cm/day);

z_o = roughness parameter (cm);

$C_T = \frac{1}{C_1 + C_2 C_H}$ = temperature coefficient;

$C_1 = 38 - (2^\circ\text{C} \times \text{elev. in m}/305)$;

$C_2 = 7.6^\circ\text{C}$;

$C_H = \frac{50 \text{ mb}}{(e_2 - e_1)}$;

e_2 = saturation vapor pressure at mean maximum temperature for warmest month of year in area (mb);

e_1 = saturation vapor pressure at the mean minimum temperature for warmest month of year in area (mb);

T = air temperature (°C);

$T_x = -2.5 - 0.14 (e_2 - e_1) ^\circ\text{C}/\text{mb} - \text{elev. (m)}/550$; and

R_s = solar radiation (ly/day).

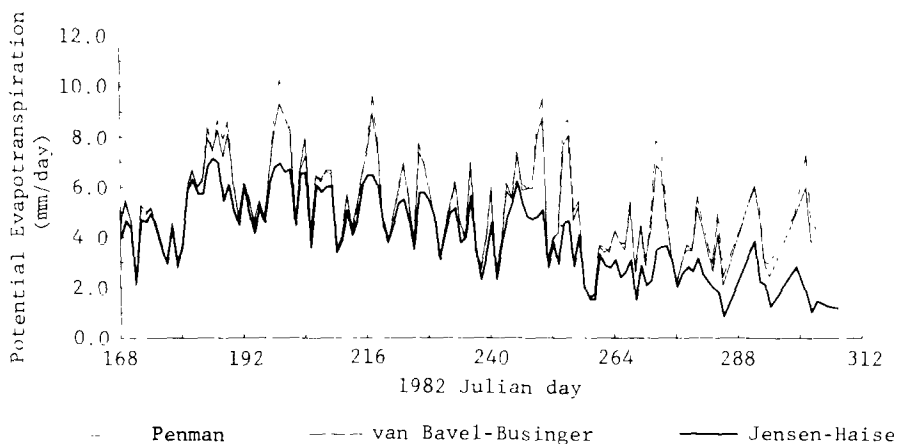


Fig. 7. Estimates of 1982 potential evapotranspiration for the Zenith site calculated by the Penman, Van Bavel-Businger and Jensen-Haise methods.

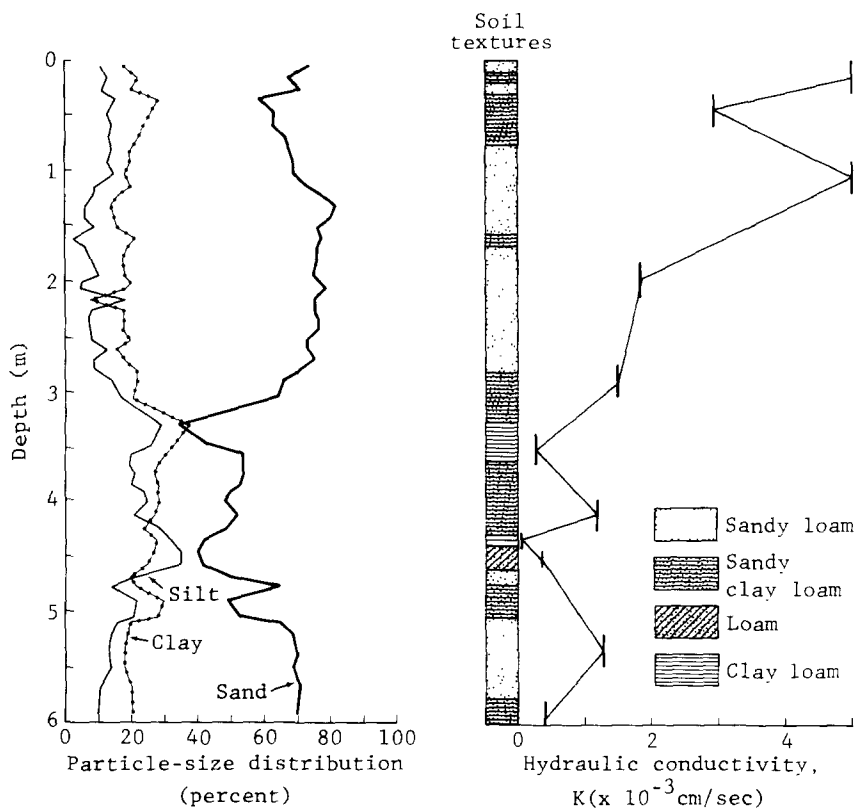


Fig. 8. Depth variation of soil-particle sizes, textures, and saturated hydraulic conductivities for Burrton site. The vertical bars indicate that the soil sample was taken from the indicated depth interval.

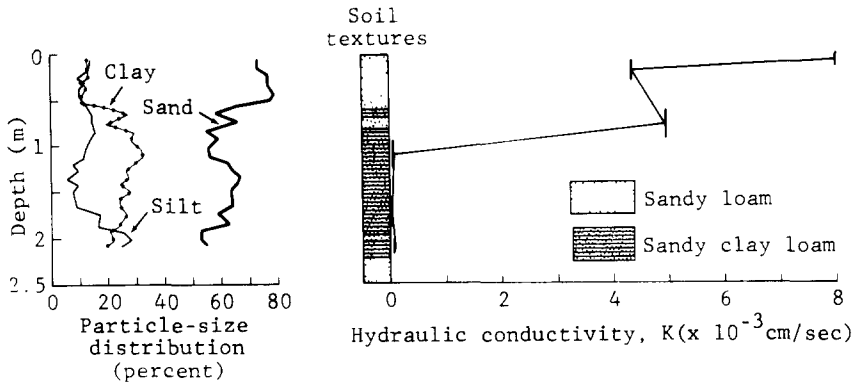


Fig. 9. Depth variation of soil-particle sizes, textures, and saturated hydraulic conductivities for Zenith site. The vertical bars indicate that the soil sample was taken from the indicated depth interval.

the two sites is of major significance in the estimated amounts of recharge in each site, as will be shown. The saturated hydraulic conductivity of the soil above the water table generally decreases with depth at both sites. This conductivity pattern is probably due to the decreasing sand content and increasing bulk density of the soil with depth.

An example of a laboratory-determined desaturation curve for a disturbed sample from the top 30.5 cm of soil at the Zenith site, together with onsite-measured pairs of neutron moistures and tensiometric pressure-head values, are shown in Fig. 10. Laboratory-derived desaturation curves were determined for a number of soil samples from different depths at each recharge site. The tensiometer data-scatter is significant, and the range of tensiometer measurements is limited to greater than -1 bar pore pressures. Because of the unconsolidated and disturbed nature of most samples, and because of the vacuum-saturation method used to saturate the samples in the laboratory, the estimated complete water saturation was higher than the maximum observed onsite-water content using the neutron probe. However, the agreement between laboratory and onsite measurements, considering all measurement errors and hysteresis effects as well as the disturbed nature of the samples, was considered to be satisfactory.

Onsite water-characteristic curves developed for the deepest tensiometers, such as 1.2 and 1.5 m at the Zenith site, are shown in Fig. 11 and are used for calculating hydraulic gradients for the reference flux in a water-balance equation that estimates water fluxes at the water table, as was explained in the "Methodology" section. Notice the limited range of tensiometer readings and the approximate nature of the empirically fitted curves due to data scatter. Given the large width of the onsite water-characteristic envelope curve (Fig. 11), such water fluxes should be considered rough estimates.

Examples of hydraulic-conductivity functions, $K(\theta)$, determined by five different methods, are shown in Fig. 12. Soil $K(\theta)$ functions in Fig. 12a

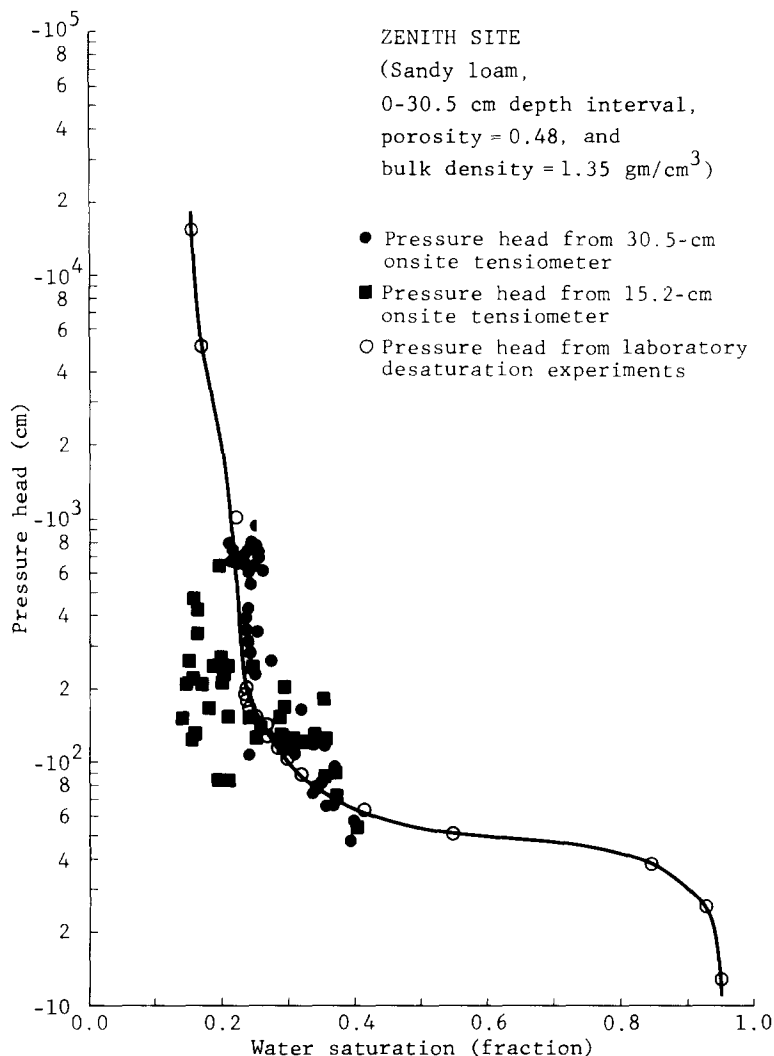


Fig. 10. Comparison of onsite- and laboratory-determined capillary pressure-head measurements for top 30.5 cm of soil at Zenith site.

correspond to the deepest tensiometer depths at the Zenith site, while the ones in Fig. 12b correspond to locations near or at the water table during recharge periods at the Burrton site. Note the sharp decrease in unsaturated hydraulic conductivity with a mild decrease in soil moisture. The horizontal portion in the Brooks and Corey curves represents the fact that the water saturation corresponding to the air-entry pressure [derived by trial and error according to the Brooks and Corey (1964) technique] is appreciably different from complete water saturation corresponding to zero capillary pressure for these particular samples. The Brooks and Corey method is based on the

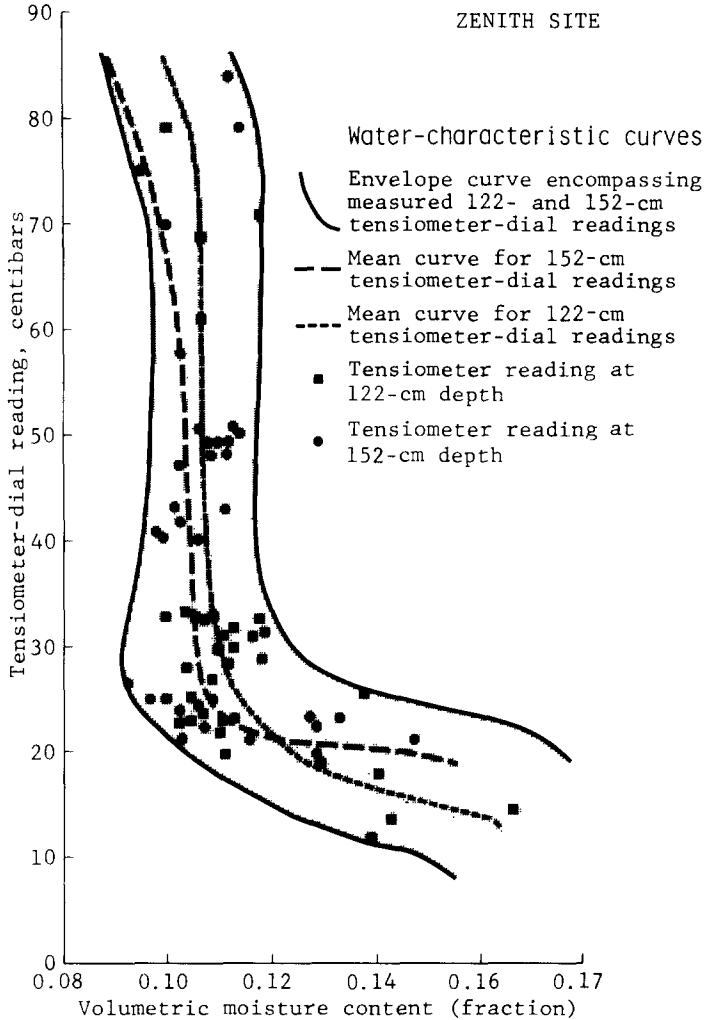


Fig. 11. Onsite water-characteristic curves for 122 and 152 cm levels at the Zenith site.

assumption that the hydraulic conductivity at capillary pressures less than or equal to the air-entry pressure is equal to the saturated hydraulic conductivity. This explains why for the range of moisture contents corresponding to the range from air-entry pressure to zero capillary pressure (full saturation), the Brooks and Corey curve is horizontal.

For the Burrton site, the average soil moisture at a depth interval of 0.3--0.9 m (which corresponds to the average depth to the water table during March to July 1983) was approximately 21%. This soil moisture corresponds to a value of unsaturated hydraulic conductivity of 0.065 cm per day using the Brooks and Corey curve (Fig. 12a). Because the average soil-moisture content at the depth interval of 1.2--1.5 m (which corresponds to the depth

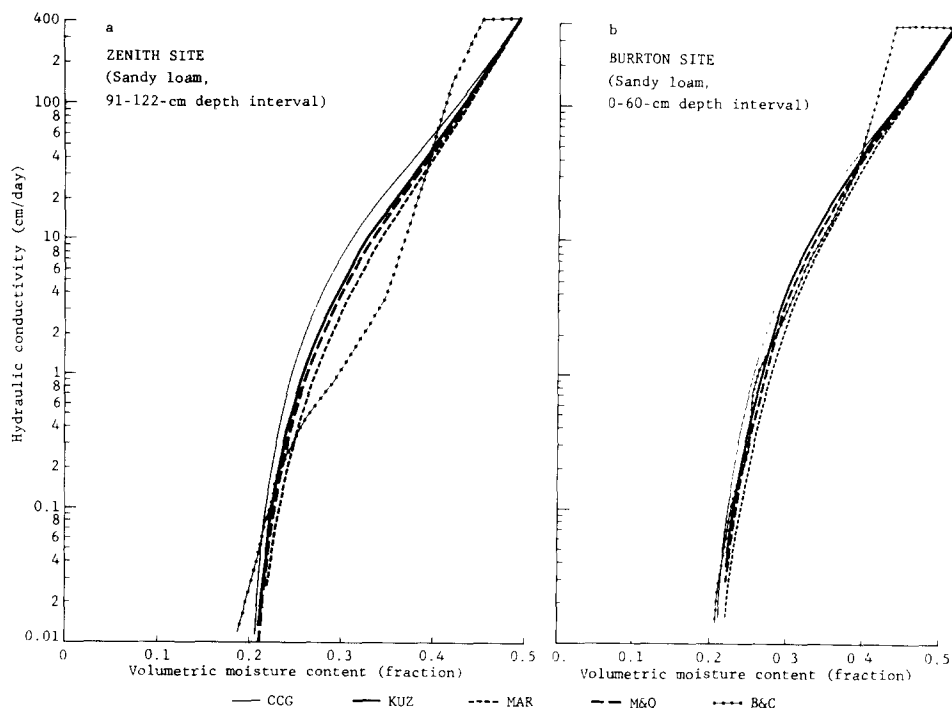


Fig. 12. Hydraulic-conductivity functions estimated using five different methods for Zenith (a) and Burrton (b) recharge sites [CCG = Childs and Collis-George (1950); KUZ = Kunze et al. (1968); MAR = Marshall (1958); M&Q = Millington and Quirk (1959, 1961); B&C = Brooks and Corey (1964) methods].

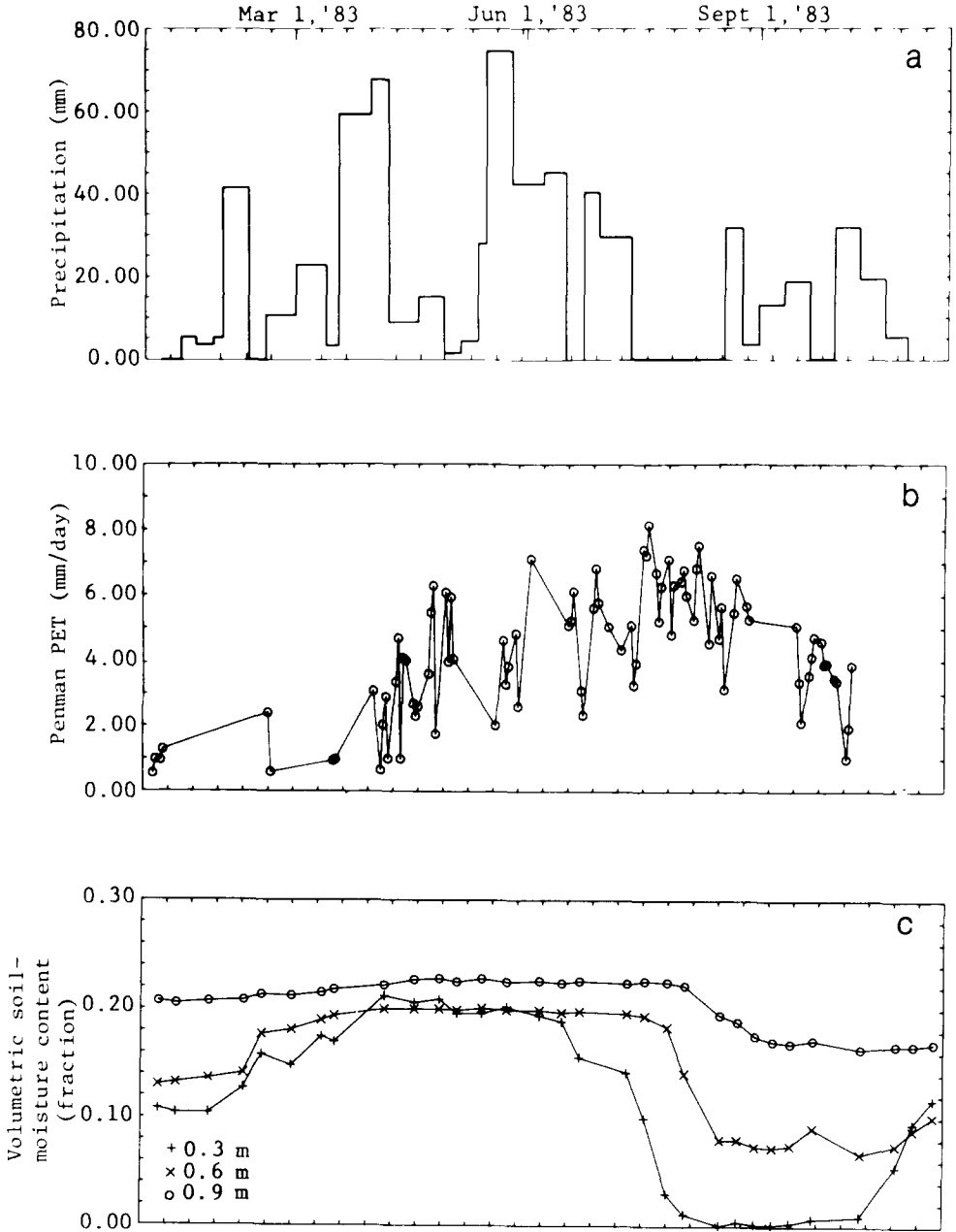
of the deepest tensiometers) was about 12.5% for the Zenith site during March to June 1983, the Brooks and Corey $K(\theta)$ curve for that depth (by extrapolating Fig. 12b by more than one log cycle) resulted in an unsaturated hydraulic conductivity of 0.0003 cm per day. This large difference in unsaturated hydraulic conductivity between the two sites will result in significant water-flux differences in those depth intervals as will be shown in the next section.

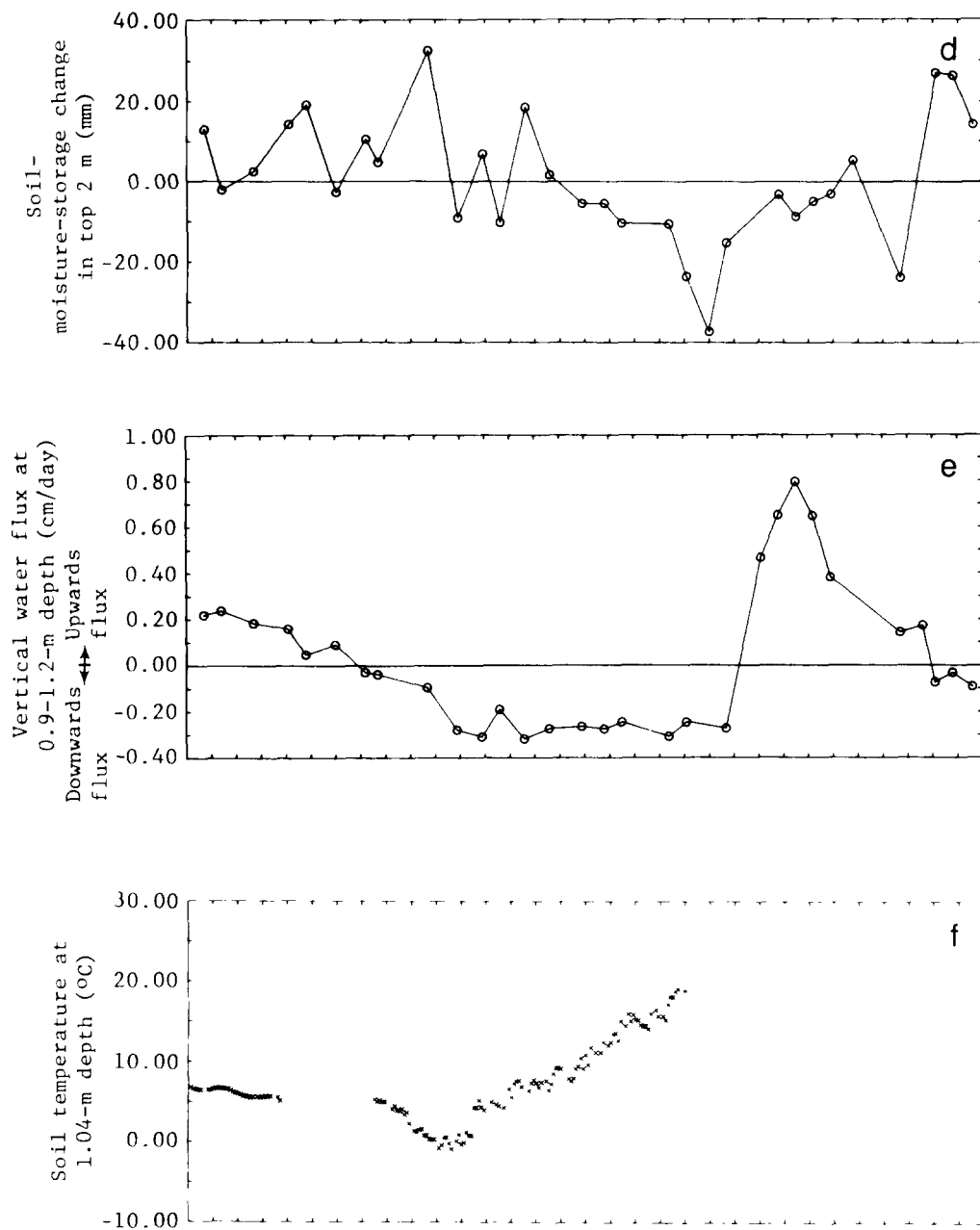
GROUNDWATER-RECHARGE ESTIMATES

Burrton site

The groundwater-recharge profile for the effective recharge period of February 10 (Julian day, JD41) to May 27 (JD147), 1983, for the Burrton site is shown in Fig. 13. During portions of this period the datalogger, which stored the hydrometeorological data for the site, failed. Therefore, the average total precipitation data from six nearby meteorological stations (shown in Fig. 1) were used for the Burrton recharge site. The distribution of

BURRTON SITE





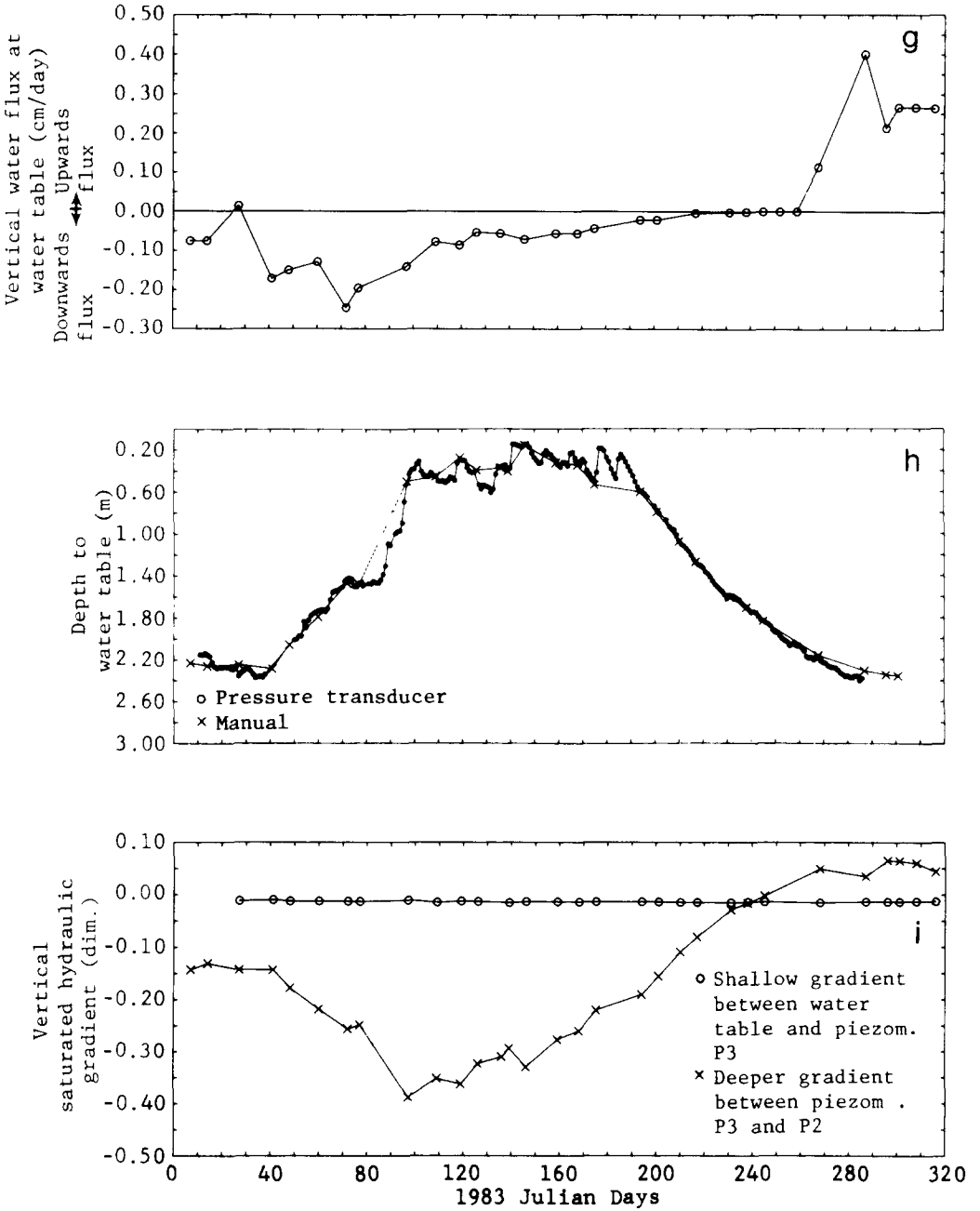


Fig. 13. Groundwater-recharge profile for the Burrton site during 1983. Time intervals lacking data symbols imply no data due to instrument malfunctions.

total precipitation over various time intervals between site visits is shown as a bar graph (Fig. 13a). The resulting volumetric moisture content at 0.3 m depth intervals for the top 0.9 m of soil is shown in Fig. 13c. The moisture content of the 0.9 m depth during the period from April to July 1983 approaches the saturated water content for that depth, since the depth to the water table was less than 1 m during that period. The moisture-storage change for the soil profile down to 2.0 m, referenced to the immediately preceding measurement and assuming that the moisture content at 0.15 m is representative of the 0–0.23 m top soil layer, is shown in Fig. 13d.

Vertical water fluxes at 0.9–1.2 m (Fig. 13e) and at the water table (Fig. 13g) indicate downward movement. This is corroborated by the depression in soil temperatures at 1.04 (Fig. 13f) and 1.34 m (not shown) due to the near-freezing temperature of infiltrating rain and snowmelt waters. As a result of flow to the water table, the water table rose nearly continuously during the effective-recharge period, as shown in Fig. 13h. The saturated hydraulic gradients near the water table (shallow gradient, Fig. 13i) are nearly constant because any rise in water level in the water-table well was accompanied by a similar water-level rise in the shallowest piezometer P3. This is in contrast with the hydraulic gradient between piezometers P3 and P2 (deeper gradient, Fig. 13i) which shows more variable gradients. The deeper piezometers did not readily respond to rises in the shallower water-table well and piezometer probably because of the increased clay content of the deeper sediments (Fig. 2). This indicates that the shallower saturated flux is influenced by precipitation much more readily than the flux indicated by the deeper piezometers. The observed water-table rises are therefore due to precipitation and not due to lateral influxes.

To support the last statement further, a study of water-level behavior in nearby observation wells (shown by triangles in Fig. 1) and at the Burrton site indicates that the wells in the area probably were not affected by irrigation withdrawals. The water levels in the nearby observation wells did not recover when irrigation pumpage stopped during September or October 1982 to January 1983, as is observed in aquifers affected by irrigation in south-central Kansas. Figure 14a for the Burrton area indicates, in a qualitative way, that water levels in nearby observation wells declined from July 1982 to January 1983 and rose from January to July 1982 and from January to July 1983. The positioning of the horizontal bars above or below the center line in Fig. 14a has no other physical significance except to indicate trends in water-level changes, not amounts of change. In cases where some wells indicate water-level increases while others indicate decreases during the same period, overlap of bars occurs in that figure. The fact that water levels declined during the summer and fall 1982 and 1983 may be attributed to the absence of effective recharge during that period. This means that for a recharge area, such as the Burrton area, a water-level decline is expected during periods without recharge. Note that no irrigation wells are located west of the Burrton site nor within 5 km north of the site.

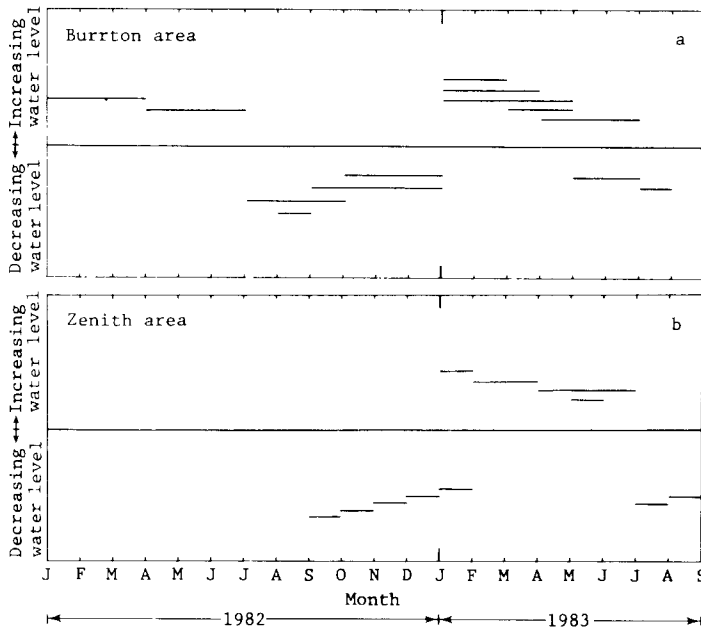


Fig. 14. Water-level changes in nearby observation wells for the Burrton (a) and Zenith (b) areas.

Irrigation wells are present south and southeast of the site, but irrigation there is fairly small, generally with water appropriations of less than $245 \times 10^3 \text{ m}^3 \text{ yr}^{-1}$ per well. Therefore, the fact that relatively few irrigation wells exist in the vicinity of the site and that their pumpage is fairly small supports the contention that the water-level observations at the site may not have been affected by irrigation pumpage.

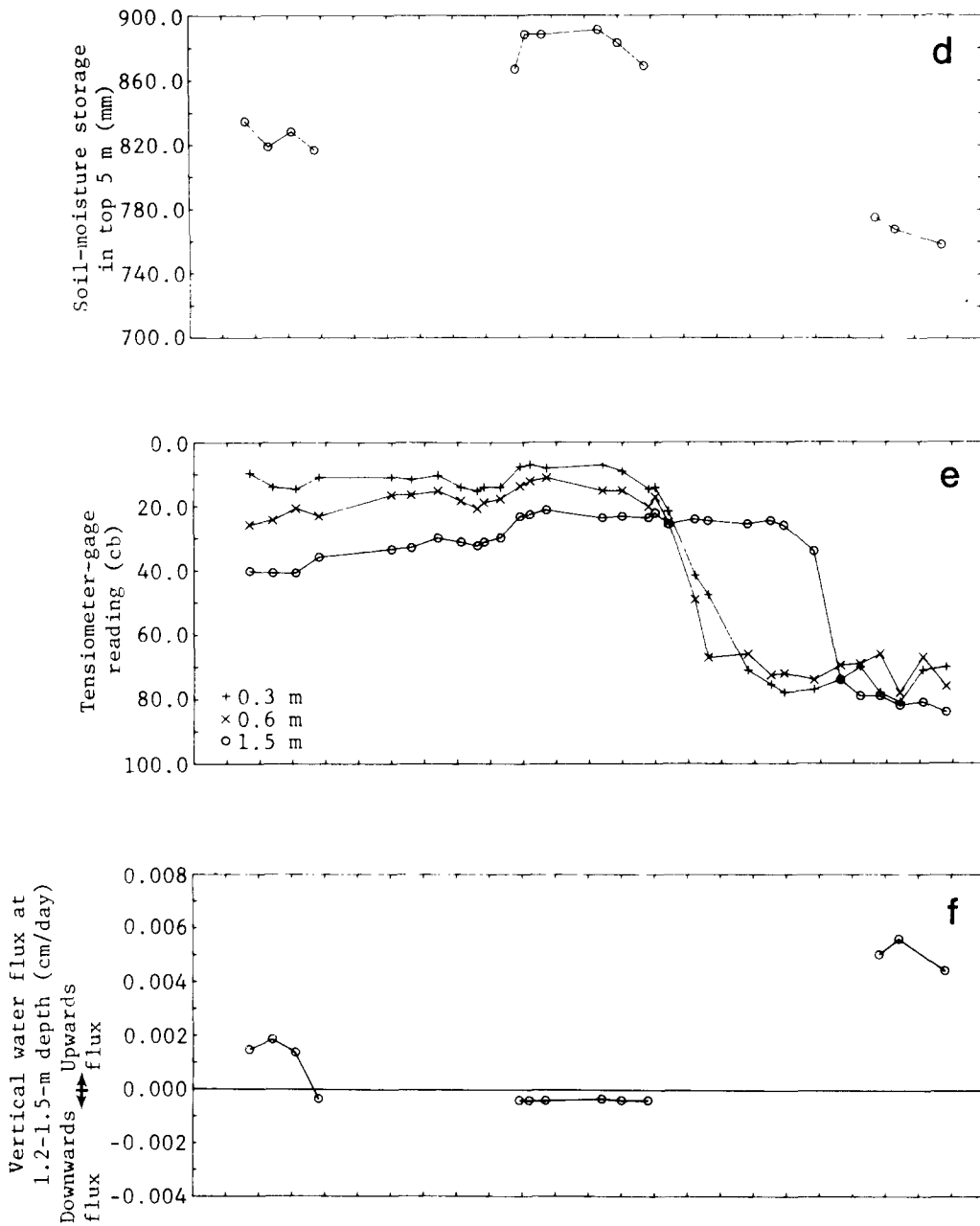
The resulting time distribution of effective recharge during February 10 (JD41) to May 26 (JD146), 1983, is shown in Fig. 13g of the recharge profile. The subsequent period of May 27 (JD147) to July 5 (JD186), 1983, although not contributing to higher water-table levels at the site, may still be considered as a recharge period in that the high water levels already achieved were maintained for the most part. After July 5 (JD186), 1983, a monotonic, consistent, and rapid water-table decline followed (Fig. 13h), which is coincident with low precipitation (Fig. 13a) and high evapotranspiration rates (Fig. 13b). During February 10 (JD41) to May 26 (JD 146), the water table rose by 2.1 m, as a result of 133.4 mm of effective recharge due to 296.9 mm of precipitation during that period. The effective-recharge estimate was calculated by summing all the products of point-flux measurements (Fig. 13g) and the length of the associated recharge-time interval, which was chosen as the midpoint interval between point-flux measurements. Snow depth on the ground during February 1–13 (JD32–44) progressively decreased from approximately 254 mm on February 2 (JD33) to 51 mm on

February 13 (JD44). Since January 1983 was mostly dry (less than 10 mm of total precipitation from January 1 to 30), the total precipitation of 342.6 mm from January 31 (JD31) to May 26 (JD146), 1983, can be assumed safely to have contributed to the calculated 133.4 mm of effective recharge. Therefore, approximately 39% of the total precipitation during January 31 (JD31) to May 26 (JD146), 1983, was inferred to have contributed to the estimated effective recharge. Subsequently, during May 27 (JD147) to July 5 (JD186), 1983, an estimated 20.6 mm of additional direct recharge to the water table resulted from 157.7 mm of rainfall.

However, a significant portion of this aquifer-recharge gain (approximately 68%; Fig. 13g) from February 10 to July 5, 1983, was lost by evapotranspiration from August to mid-November. During the summer and fall of 1983, the evaporation front propagated progressively deeper in the soil profile, as can be seen by the drying of the soil profile during that period (Fig. 13c), the negative successive soil-moisture changes in the soil profile (Fig. 13d), and the strong upwards water flux in the 0.9–1.2 m soil layer (Fig. 13e), which eventually propagated downwards to the water table (Fig. 13g). Note the time lag and attenuation of the evaporation front as it propagates from approximately 1 to 2 m depth, as shown in Figs. 13e and g, respectively. Also note the reversal of the saturated hydraulic gradient (Fig. 13i) between piezometers P2 (screened at ~ 17 m) and P3 (screened at ~ 12 m) from September to November 1983, indicating a transformation from a recharge to a discharge regime at the P3–P2 depth interval during the fall of 1983. However, such a reversal was not observed during the fall of 1982.

Zenith site

The groundwater-recharge profile for the effective recharge period of April 7 (JD97) to June 29 (JD180), 1983, for the Zenith site is shown in Fig. 15. Because the data logger malfunctioned during most of the period from July 1983 onwards, precipitation values from the Hudson meteorological station, approximately 21 km northwest of the site (Fig. 1), were employed to supplement the Zenith site record after July 3 (JD184), 1983 (Fig. 15a). Two distinct periods of effective recharge can be recognized during this time interval. The first one caused a water-table rise of 0.17 m during April 7 (JD97)–12 (JD102), 1983 (Fig. 15h). This recharge event resulted from almost daily precipitation from March 19 (JD78) to April 12 (JD102), 1983, totaling 85.9 mm (Fig. 15a). The water flux at the 1.2–1.5 m level, based on tensiometer readings, was downward, totaling less than 0.1 mm during this six-day period. The flux at the water table during this same period (Fig. 15g) could not be estimated because of a malfunction of the neutron probe. This first period of recharge was followed by a water-table decline, reaching its lowest point on May 19 (JD102), 1983 (Fig. 15h). After April 12 (JD102), precipitation was not as frequent, reaching a total



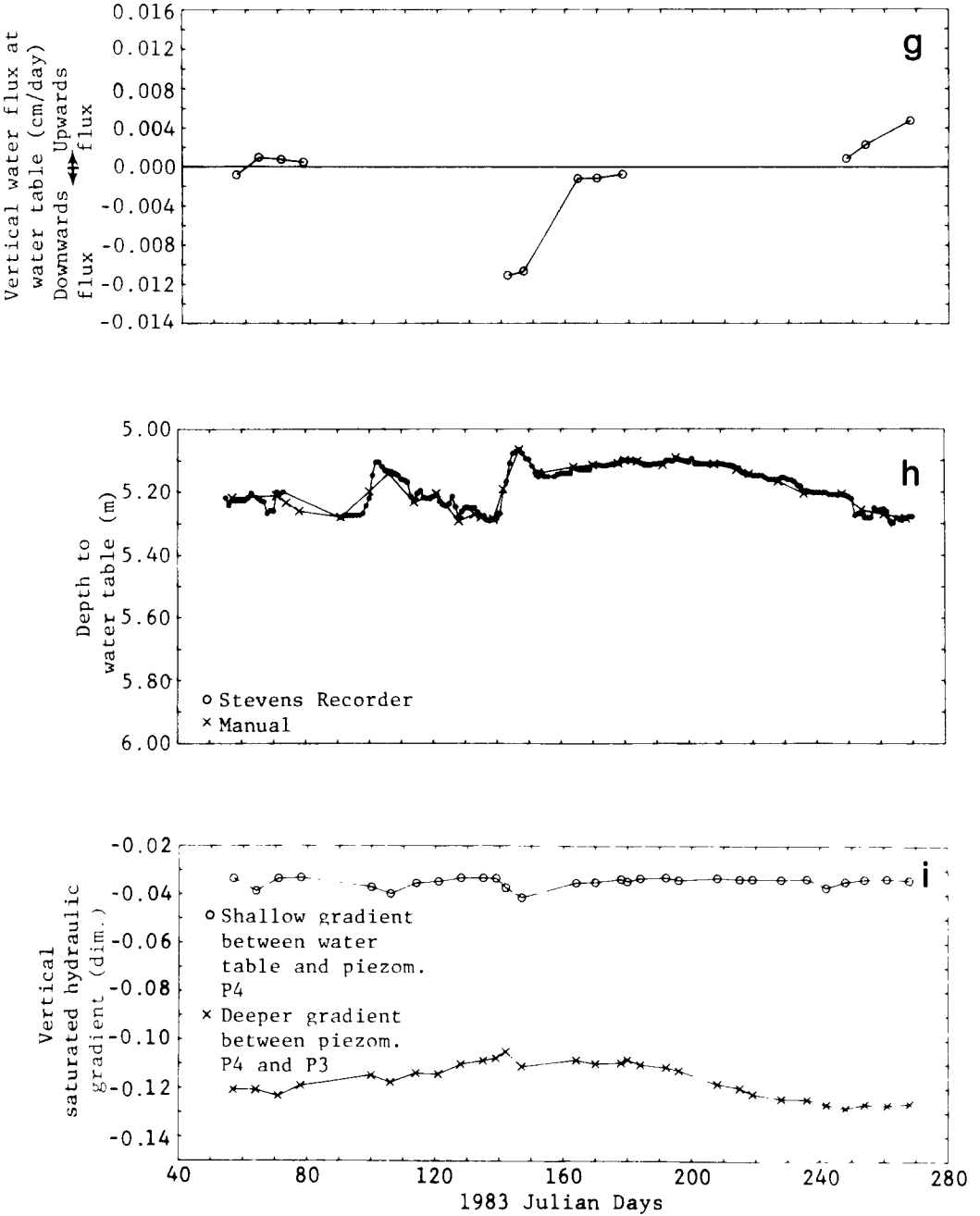


Fig. 15. Groundwater-recharge profile for the Zenith site during 1983. Time intervals lacking data symbols imply no data due to instrument malfunctions.

of 20.1 mm by April 30 (JD120), followed by no precipitation up to May 16 (JD136), 1983 (Fig. 15a).

The second period of recharge caused a water-table rise of 0.22 m from May 19 (JD139) to May 27 (JD147) and resulted from 72.9 m of precipitation during May 17–27 (JD137–147). The flux at the water table during this second recharge period totaled approximately 0.9 mm. This rise in the water table was followed by a small decline (Fig. 15h) until June 4 (JD155), 1983, after which a gradual, small rise (0.05 m) in the water table was observed until approximately June 29 (JD180), 1983, probably due to 63.0 mm of precipitation from May 28 (JD148) to June 13 (JD164), 1983; only 8.1 mm of rain occurred after that until June 29 (JD180). Although the two relatively sharp water-table rises observed at the Zenith site (Fig. 15h) most probably were caused by local recharge, the gradual water-table rise from June 4 to 29 (JD 155–180), 1983, was probably due to a combination of local recharge and regional flow from the west (refer to Figs. 4 and 14b) because a gradual water-level rise during this period was observed at the deeper piezometers (P2, P3, P4) as well, without any noticeable time lag in the piezometer responses. Rainfall amounts for June, 1983, were lowest at the site (67.0 mm), increasing westwards with 84.8 mm at Pratt, ~45 km southwest; 108.7 mm at Trousdale, ~58 km west-southwest, and 167.9 mm at Larned, ~60 km west-northwest from the Zenith site.

The water table started slowly declining after June 29 (JD180), 1983 (Fig. 15h). This water-table decline is coincident with the drying soil profile (Figs. 14c, d, and e) and upward moisture flows (Figs. 15f and g). The flux at the water table during May 28 (JD148) to June 29 (JD180) was approximately 1.2 mm (Fig. 15g). Thus, a total of 2.1 mm of recharge occurred during May 19 (JD139) to June 29 (JD180) as a result of 153.9 mm of precipitation since May 17 (JD137). Thus, only 1.4% of this precipitation resulted in recharge. As was also observed at the Burrton site, a portion (although smaller than at Burrton) of this aquifer-recharge and soil-moisture-storage gain was lost by evaporative fluxes during August through October 1983, as can be seen from Figs. 15c through h.

The hydraulic head gradient near the water table (Fig. 15i) was fairly constant during the period of record with two peaks coinciding approximately with the two above-mentioned recharge periods. The hydraulic head gradient between piezometers P4 at 23 and P3 at 31 m depth shows an increase during summer and fall due to the steeper water-level decline in the deeper piezometer P3 compared to that of P4, which follows the water-table decline more closely. The thick clay layer between piezometers P4 and P3 (Fig. 2) seems the likely reason for this observation. The nearby observation wells (Fig. 1) at the Zenith site show a consistent water-level rise from January to June 1983 followed by a water-level decline (Fig. 14b).

Comparison of recharge estimates and some sources of error

The large difference between the estimated recharge at the Zenith site (2.1 mm) and the estimated recharge at the Burrton site (154 mm) was unexpected. Therefore, to check this result, the hydraulic conductivity corresponding to the average moisture content at the 0.9–1.2 m depth interval at the Zenith site (see section on “Soil hydrogeologic properties”) and thus the reference-flux values at the same depth interval were increased by one order of magnitude. Equation (2) then was employed to calculate the fluxes at the water table during the May 19 to June 29 (JD139–180), 1983, recharge period. The resulting recharge amount of 3.0 mm during this time interval amounted to approximately 2.0% of the total precipitation (153.9 mm) during the same time interval, compared to approximately 1.4% previously, a number which still is very small compared to the recharge estimate at the Burrton site.

Also during the major recharge period of March 1 (JD60) to June 30 (JD181), 1983, precipitation was higher for the Burrton site — 414 mm (Fig. 13a) than for the Zenith site — 255 mm (Fig. 15a), and the estimated average daily PET during the same time period was higher for the Zenith site — 4.4 mm per day (Fig. 15b) than for the Burrton site — 3.7 mm per day (Fig. 13b). Finally note that the approximate average soil-moisture storage in the top 1.2 m was higher (265 mm) for the Burrton site than for the Zenith site (193 mm) due to the shallower water table at the Burrton site (Fig. 13h versus Fig. 15h). As a result, the average volumetric moisture content for the top 1.2 m of soil for the Burrton site was approximately 21.7 versus 15.8% for the Zenith site. Although precipitation at the Zenith site during this period was approximately 62% of the precipitation at the Burrton site, the estimated recharge for the Zenith site amounted to less than 1.5% of that estimated for the Burrton site. The fact that the hydraulic conductivity decreases by several orders of magnitude from saturation to near dryness (Fig. 12 for example) may help explain the large differential in estimated recharge values between the two sites.

The reliability of groundwater-recharge estimates depends on the accuracy of estimated soil-water-characteristic functions and unsaturated hydraulic-conductivity functions for the vadose zone. Soil-water measurements with a neutron probe can be precise to less than 1% with correct use. The main sources of error in neutron-probe usage are inaccurate calibration, soil damage from access-tube installation, damage to surface soil and vegetation, water traveling along the access tube or seeping into the access tube, relocation error, random-count error, large temperature differential between the probe that is lowered into the access tube and the surface unit containing counting and display circuits, batteries, etc. in a closed metal box, and inherent soil variability. Sources of error in tensiometry are entrapped air bubbles and leaks, variations with temperature, loss of porous-cup contact with the soil, water traveling along the shaft, and parallax.

Hysteresis effects preclude accurate determination of onsite water-characteristic curves for the unsaturated zone. The error is probably further compounded by the use of mean characteristic curves to translate neutron moisture readings to hydraulic-head values. Determination of unsaturated hydraulic-conductivity functions, as was mentioned earlier, is difficult and time consuming both onsite and in the laboratory, with the difficulty and uncertainty increasing with increasing soil dryness. These problems are compounded by the inherent large degree of spatial variability, which precludes the application of the hydraulic-conductivity function for a given soil to any other location. Because neither replicate hydraulic conductivity or desaturation experiments were conducted on the same samples nor were sufficient samples from the same depth interval collected and analyzed for these physical properties, quantified statistical error analysis could not be performed. Furthermore, because no onsite hydraulic-conductivity experiments for comparison with laboratory experiments were conducted, assessment of the hydraulic conductivity error component was not attempted. The key to increasing reliability of groundwater-recharge estimates lies with the conductivity determinations. Because of the above-mentioned sources of error, recharge estimates such as the ones presented here should only be considered as rough approximations.

Conditions under which recharge takes place

A certain amount of moisture build-up in the soil zone, which is influenced by evapotranspiration, is needed for effective groundwater recharge to occur. In a comprehensive study on the mechanisms of groundwater recharge, Freeze (1969) concluded that of all the factors controlling groundwater recharge, the antecedent soil-moisture regime probably is the most important. Figure 16 presents the driest and wettest soil-moisture profiles for both recharge sites, as well as the moisture profiles just prior to effective recharge. The driest profiles, which occurred after a long period of little or no precipitation and high evapotranspiration, may be considered as *approximating* residual-moisture profiles, that is, minimum-moisture profiles after the effects of gravity drainage and evapotranspiration become negligible. The moisture profiles observed just before effective recharge was initiated may be reasonably assumed to have reached their water-holding capacity.

The latter part of November to mid-February represents the period during which the already-dry moisture profiles effectively build up moisture at the Burrton site. The January and early February 1983 moisture profiles can be reasonably assumed to closely approximate their water-holding capacity, which in water-depth-equivalent terms for the top 2 m of the profile totals about 368.9 mm. Since the driest observed profile of October 14 (JD287), 1983 (Fig. 16), can be assumed to represent the residual moisture profile totaling 260.9 mm, the moisture build-up required before initiation of effective recharge for Burrton is approximately 108 mm.

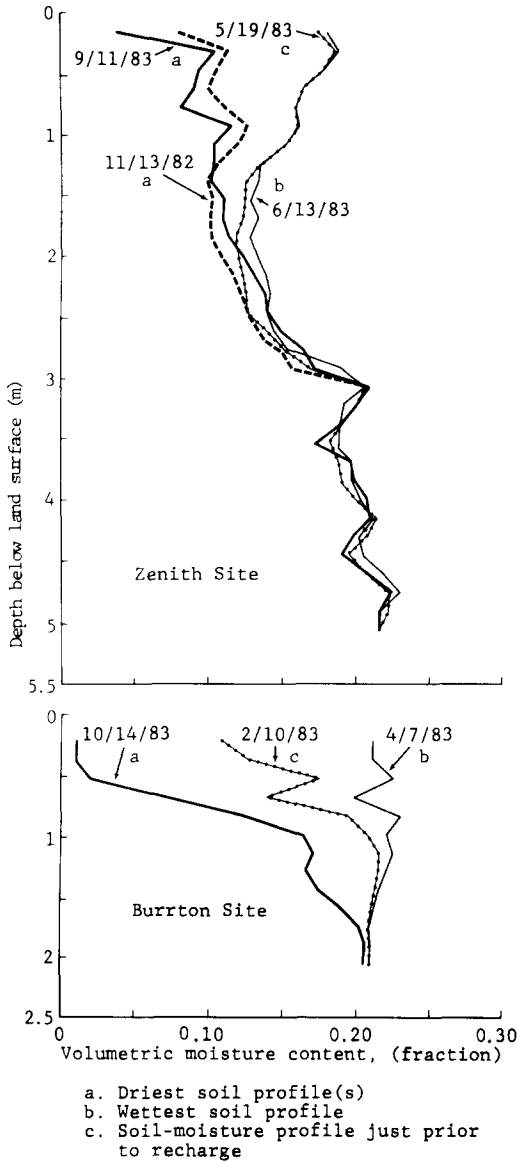


Fig. 16. Driest and wettest observed soil-moisture profiles during 1982-83 for Zenith and Burrton recharge sites.

For the Zenith site with the longer unsaturated soil profile (approximately 5.03 m), the overall choice of the driest or wettest profile is made by calculating the equivalent depth of water stored in the entire profile. This choice is made because individual sections of the soil profile may be wetter or drier than the selected one at different times. The driest profiles for both

1982 and 1983 for the Zenith site are indicated in Fig. 16. The November 1982 profile represents the driest one for the 4–10 m depth interval, while the September 1983 profile represents the driest one for the 0–4 m depth interval. The moisture mounding at approximately the 2.4 m level (Fig. 16) above the sandy clay loam and clay loam layers (Fig. 9), even during the 1983 driest overall profile, indicates the partially confining nature of that layer. Mid-November to March represents the period of effective soil-moisture build-up for the Zenith site. Note that during this time period, evapotranspiration-moisture losses are at their minimum (Fig. 15b). The May 1983 moisture profiles can be assumed to closely approximate their water-holding capacity, which in depth-water-equivalent terms totals about 881.4 mm. Since the driest overall moisture profile of September 11 (JD754), 1983 (Fig. 16), can be assumed to approximate the residual-moisture profile totaling approximately 767.0 mm, the moisture build-up required for initiation of effective recharge for Zenith is approximately 114.4 mm. The generally sandier nature of the Zenith soil profile (Fig. 9) down to the 3 m depth level and the nearly constant moisture distribution beyond that depth during the study period may help explain the relatively low moisture build-up required for the Zenith profile before effective recharge can take place.

Over most of the duration of this study, the moisture profiles in general were nearly constant below approximately 0.9 m for Burrton and 2.7 m for Zenith, with both depth levels corresponding to a transition from sandy loam to sandy clay loam. In general, evapotranspiration losses below these depths were relatively minor. However, under severe dryness these evapotranspiration depth levels could move downwards as was observed, particularly at the Burrton site, during the dry period of July through October 1983 (Fig. 13).

The most effective way to build up soil moisture in the profile is through frequent rainfall over a period of time with relatively small evapotranspiration losses, such as during winter and early spring. In addition to rainfall, snowmelt is effective in building up soil moisture. For example, the first recharge period observed at the Burrton site during mid-February 1983 was due predominantly to the melting of accumulated snow on the ground at the site. During site visitation, a snow depth of approximately 177.8 mm was observed on February 10, 1983 (JD41), and no snow was observed on February 17, 1983 (JD48). During this period no precipitation at the site or on the surrounding area was reported. Also freezing temperatures were recorded at the site and in the general area up to February 10 (JD41); after which snowmelt started. The observed soil-moisture and water-table rises during this and subsequent periods, together with the unusually depressed soil temperatures observed after snowmelt (Fig. 13f), support these observations.

Heavy summer rains or thunderstorms at both recharge sites did not contribute to recharge during the study period. The effect of summer and

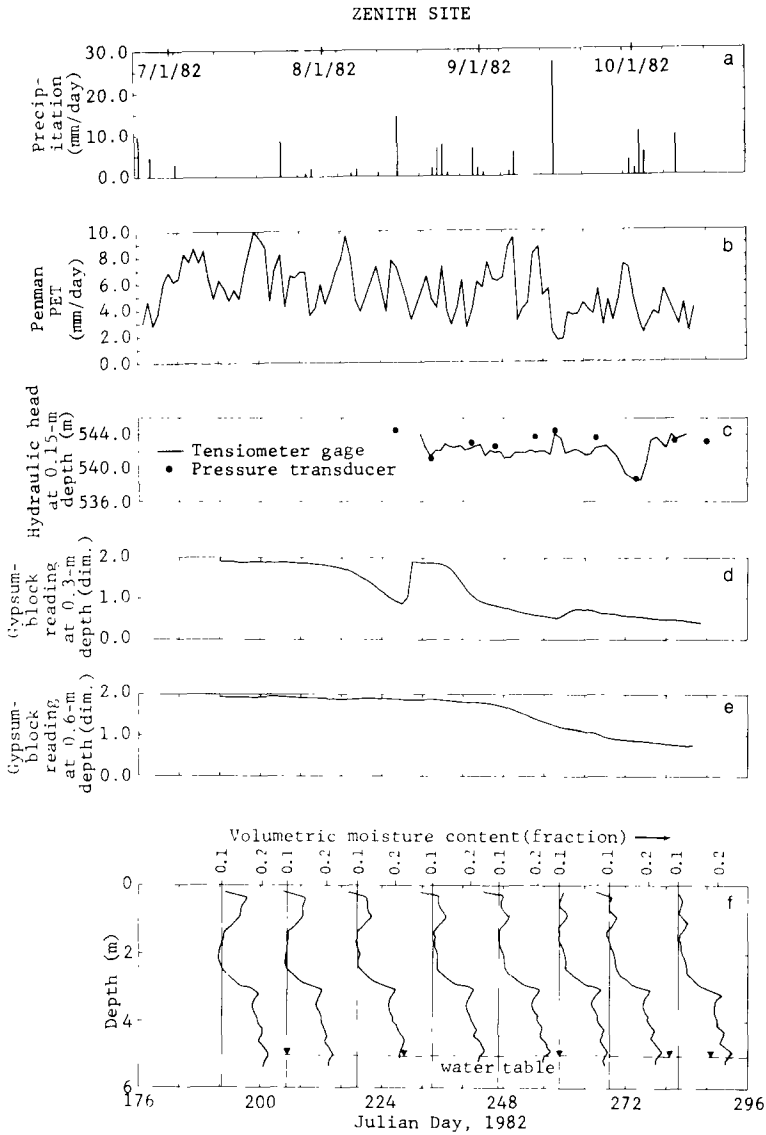


Fig. 17. Effect of summer and fall 1982 rains on groundwater recharge for Zenith site.

fall rain for July 1 (JD182) to October 15 (JD259), 1982, at the Zenith recharge site, for example, is analyzed in Fig. 17. Two major storms occurred during this period (Fig. 17a), one on August 16 (JD228), totaling 15.0 mm, and one on September 16 (JD259), totaling 28.2 mm. These storms clearly penetrated only the top 0.3 m of the soil profile at the Zenith site and did not affect the 0.6 m depth level as can be clearly seen by observing the gypsum block response at the 0.3 and 0.6 m depth (Figs. 17d and e). At both

sites the excess water during the storms was observed to accumulate in numerous shallow depressions, thus forming ephemeral ponds which evaporated quickly under the prevailing high potential-evapotranspiration environment (Fig. 17b). The tensiometer-transducer data for 0.15 m depth averaged over a daily period together with time-instant dial-gage readings also are shown (Fig. 17c). Soil moisture depletion during the hot, dry periods of summer and the temporary moisture build-up during storms also are shown in Fig. 17f.

Longer duration high- or low-intensity rainfalls may contribute to effective groundwater recharge. For example, the high-frequency and high-intensity rainfall combination at the Burrton site during March 26 (JD85) to April 5 (JD95), and May 11 (JD131) to May 29 (JD149), 1983, contributed substantial amounts of effective groundwater recharge. The almost daily rainfall at the Zenith site during March 19 (JD78) to April 12 (JD102), 1983, contributed to effective recharge on April 7–12. Note that the second observed period of effective recharge at Zenith during May 19–28 (JD139–148), 1983, was not preceded by a high-frequency rainfall but was caused almost solely by a practically continuous 24 h rainfall totaling 58.9 mm on May 20 (JD140). The resulting water-table rise was maintained by frequent high-intensity rainfall immediately following from May 30 (JD150) to June 13 (JD164).

If one considers the record of Hutchinson 10SW Meteorological Station (Fig. 1), which is approximately equidistant between the two sites, as representative of precipitation at the study sites, then that station's 1982 total precipitation of approximately 675.6 mm is below the 1960–1983 average of 729.0 mm, while the 1983 total precipitation of 784.9 mm is above average. The major moisture build-up during December 1982 through February 1983 at both sites and at nearby meteorological stations was characterized by above-average precipitation (113.3 mm average in the Hutchinson 10SW station versus 71.4 mm normal average for 1898–1961) and contributed to the observed 1983 recharge at both sites.

CONCLUDING REMARKS

The main objective of this study, that is the determination of the amount and time distribution of groundwater recharge from precipitation at two specific sites in south-central Kansas, has been achieved. Recharge occurred only during late winter and spring; no recharge occurred in late summer and fall, and the estimated recharge amounts were significantly different for the two recharge sites, ranging from approximately 154 mm at Burrton to less than 2.5 mm at Zenith. However, a significant portion of this predominantly springtime recharge was lost by evapotranspiration during late summer and fall, especially at the Burrton site (68%) because of its very shallow water table. Both sites are located in sand-dune areas in natural

groundwater-recharge areas (as opposed to discharge areas) with similar sandy soils characterized by underlying, relatively thin clayey layers, typical of south-central Kansas. The reader is cautioned against generalizing the estimated recharge amounts found in this study over large areas because such results represent only two relatively short-term point measurements in the extensive sand-dune areas of south-central Kansas. Again, the recharge estimates presented here should only be regarded as approximate.

Soil layering in the unsaturated zone, such as the progression from sandy loam to sandy clay loam to clay loam at the Zenith site (Fig. 9), plays an important role in facilitating or restricting downward water movement to the water table, as was mentioned previously. Also, given that the soils at both sites are similar, the depth to the water table is important in groundwater-recharge estimations. The main cause of the large differential in recharge estimates observed at the two sites is the greater thickness of the unsaturated zone, as well as the lower average moisture content in that zone for the Zenith site. The lower precipitation and higher potential evapotranspiration for the Zenith site contributed to the lower soil-profile moisture content. This lower moisture content resulted in a corresponding decrease in the average unsaturated hydraulic conductivity compared to the average unsaturated hydraulic conductivity at the Burrton site.

For studies such as this one, where hysteresis effects have not been analyzed in detail, calculation of water fluxes in the unsaturated zone based on site-derived "average" water-characteristic curves may be more advantageous than using raw tensiometer data for flux calculations. Also for cases of predominantly vertical unsaturated water fluxes and a measured reference water flux in the upper soil profile, simple integration of the one-dimensional water-balance equation was found to be an effective way of translating an upper-layer flux to a deeper-water flux at the water table. This procedure, however, requires a neutron-probe access tube penetrating below the water table and its expected range of fluctuation. The combination of water-characteristic curves and saturated hydraulic conductivities provided a relatively simple way of predicting the unsaturated hydraulic-conductivity functions used in this study, given that the onsite water contents at the soil depths at which flux calculations were carried out were not near the extreme-dry moisture ranges and that the soils were not too clayey.

ACKNOWLEDGMENTS

We gratefully acknowledge Nadeem Shaukat, student research assistant with the Kansas Geological Survey, who ably assisted in all phases of this study. Dwight Hoxie of the U.S. Geological Survey and an anonymous reviewer provided valuable comments on the manuscript.

REFERENCES

- ASTM (American Society for Testing Materials), 1979. 1979 Annual Book of ASTM Standards. Part 19. Am. Soc. Test. Mater., Philadelphia, Pa., 632 pp.
- Black, C.A., 1965. Methods of Soil Analysis. Part 1. Am. Soc. Agron., Madison, Wisc., 770 pp.
- Brooks, R.H. and Corey, A.T., 1964. Hydraulic properties of porous media. Colorado State University, Ft. Collins, Colo., Hydrol. Pap. No. 3, 27 pp.
- Childs, E.C. and Collis-George, N., 1950. The permeability of porous materials. Proc. R. Soc. London, A(201): 392-405.
- Duke, H.R., 1972. Capillary properties of soils — influence upon specific yield. Trans. Am. Soc. Agric. Eng., 15(4): 688-691.
- Freeze, R.A., 1969. The mechanism of natural ground-water recharge and discharge: 1. One-dimensional, vertical, unsteady, unsaturated flow above a recharging or discharging groundwater flow system. Water Resour. Res., 5: 153-171.
- Freeze, R.A. and Banner, J., 1970. The mechanism of natural ground-water recharge and discharge: 2. Laboratory column experiments and field measurements. Water Resour. Res., 6: 138-155.
- Howard, K.W.F. and Lloyd, J.W., 1979. The sensitivity of parameters in the Penman evaporation equations and direct recharge balance. J. Hydrol., 41: 329-344.
- Jackson, R.D., Reginato, R.J. and Van Bavel, C.H.M., 1965. Comparison of measured and calculated hydraulic conductivities of unsaturated soil. Water Resour. Res., 1: 375-380.
- Jensen, M.E., 1973. Consumptive use of water and irrigation water requirements. Am. Soc. Civ. Eng., 215 pp.
- Jensen, M.E. and Haise, H.R., 1963. Estimating evapotranspiration from solar radiation. Am. Soc. Civ. Eng., J. Irrig. Drain. Div., 89: 15-41.
- Kansas Geological Survey, 1964. Geologic map of Kansas. Kans. Geol. Surv. Map M-1, scale 1:500,000.
- Kimball, B.A. and Jackson, R.D., 1975. Soil heat flux determination: a null alignment method. Agric. Meteorol., 15: 1-9.
- Kunze, R.J., Uehara, G. and Graham, K., 1968. Factors important in the calculation of hydraulic conductivity. Soil Sci. Soc. Am., Proc., 32: 760-765.
- Marshall, T.J., 1958. A relation between permeability and size distribution of pores. J. Soil Sci., 9: 1-8.
- Millington, R.J. and Quirk, J.P., 1959. Permeability of porous media. Nature, 183: 387-388.
- Millington, R.J. and Quirk, J.P., 1961. Permeability of porous solids. Trans. Faraday Soc., 57: 1200-1207.
- Nielsen, D.R., Biggar, J.W. and Erh, K.T., 1973. Spatial variability of field measured soil-water properties. Hilgardia, 42(7): 215-259.
- Penman, H.L., 1948. Natural evaporation from open water, bare soil and grass. Proc. R. Soc. London, A193: 120-146.
- Penman, H.L., 1963. Vegetation and hydrology. Commonwealth Bureau of Soils, Technol. Comm. No. 53, Harpenden, 125 pp.
- Rockers, J.J., Ratcliff, I., Dowd, L.W. and Bouse, E.F., 1966. Soil survey of Reno County, Kansas. U.S. Dep. Agric., Soil Conserv. Serv., 72 pp.
- Rose, C.W., Stern, W.R. and Drummond, J.E., 1965. Determination of hydraulic conductivity as a function of depth and water content for soil in situ. Aust. J. Soil Res., 3: 1-9.
- Shaukat, N. and Sophocleous, M.A., 1983. Evaluation of predictive methods of hydraulic conductivity based on porous media properties. Kans. Geol. Surv., Open-File Rep. 83-31.

- Sophocleous, M.A., 1985. The role of the unsaturated zone in ground-water-recharge estimations: A numerical study. *Ground Water*, 22(1): 52–58.
- Sophocleous, M.A. and Perry, C.A., 1984. Experimental studies in natural groundwater recharge dynamics: Assessment of recent advances in instrumentation. *J. Hydrol.*, 70: 369–382.
- Van Bavel, C.H.M., 1966. Potential evaporation: The combination concept and its experimental verification. *Water Resour. Res.*, 2(3): 455–467.
- Van Bavel, C.H.M., Stirk, G.B. and Brust, K.J., 1968. Hydraulic properties of a clay loam soil and the field measurement of water uptake by roots: I. Interpretation of water content and pressure profiles. *Soil Sci. Soc. Am., Proc.*, 32: 310–317.
- Warrick, A.W. and Nielsen, D.R., 1980. Spatial variability of soil physical properties in the field. In: D. Hillel (Editor), *Applications of Soil Physics*. Academic Press, New York, N.Y., pp. 319–344.